Classes of Sub-Miniature Microwave Printed Circuit Filters with Arbitrary Passband and Stopband Widths

BRIAN J. MINNIS

Abstract —**Four new classes of microwave bandpass filters are defined herein. They are realized in triplate stripline and are exceedingly small devices as a result of using transmission line elements which are a quarter-wavelength well above the frequency of the passband. Each filter corresponds to a bandpass S-plane prototype which is derived using exact synthesis procedures from a specification of transmission zero locations. Passband and stopband widths may be independently specified and an extremely high degree of selectivity can be achieved when necessary. The slope of a filter skirt can be chosen to be such that 60 dB of attenuation is reached at a frequency < 3 percent from the corner of the passband.**

I. Introduction

MODERN MICROWAVE receiver systems have a clear requirement for small, highly selective, bandpass filters whose passbands and stopbands can be independently specified and, most importantly, whose phase and amplitude characteristics are closely consistent within batches of the same device. Four new classes of bandpass filters have been recently defined which together cover these requirements. They are printed circuit devices to give the necessary performance tracking, and are constructed in triplate stripline to give low loss and low cost of manufacture.

Most common bandpass filters realized in triplate consist of capacitively or directly coupled transmission lines, one quarter-wavelength long at the center of the passband. They can be derived from highpass S-plane prototypes using the Richards transformation [1] $S = j\tan(\pi f/2f_0)$, where f and S are the real and complex frequency variables respectively, and f_0 is the center frequency of the passband. The high-pass characteristic of the prototype becomes a periodic bandpass characteristic in the f-plane as a result of the change in sign of the reactance of all the resonators at f_0 and all multiples of f_0. The stopband width is thus determined by the specified passband width. To permit independent specification of the width of pass and stopbands, a bandpass S-plane prototype can be synthesized so that in the f-plane a periodic bandpass characteristic can be achieved with all the transmission line resonators a quarter-wavelength at the center frequency of the stopband. The frequency transformation is illustrated in Fig. 1. As a further bonus, such filters will be physically small as a result of the reduction in length of the resonators. All the classes of filter to be described will correspond to bandpass

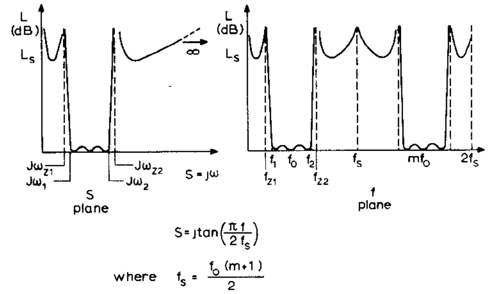

Fig. 1. Richards transform for BP prototypes.

prototypes in the S-plane. They will be classified in terms of their prototypes.

At one time the synthesis by exact procedures of LP, HP, or BP S-plane prototypes with prescribed insertion characteristics was a considerable problem both in theoretical and computational terms. This is not the case today, now that exact synthesis procedures are well established [2], [3] and modern computers offer the necessary speed and precision. However, the availability of such techniques does not render the design of practical microwave filters a fait accompli. The equally significant task of identifying classes of S-plane prototypes which correspond to physically realizable filters for a useful range of electrical specifications still remains, and is by no means trivial. It is in this regard that this paper makes its contribution. Of a number of classes of prototype identified, the four which are to be described and designated A, B, C, and D are relevant for triplate. They enable filters to be designed for passband widths in the range 10–100 percent and stopband widths which correspond to the specification of the next higher order passband at up to seven times the center frequency of the first.

To demonstrate the design procedures, a number of experimental bandpass filters have been constructed, two of which are shown in Figs. 2 and 3. The first has a 4–8-GHz passband with a stopband extending to 28 GHz and the second has a 2–6-GHz passband with a stopband extending to 22 GHz. They are very much smaller than the alternative LP/BP combinations of more conventional filters that would be required for the same electrical specifications, and they are found to be extremely consistent in manufacture. The circuits are etched on one side of a double-sided copper clad dielectric material using conventional photolithographic techniques and require no short

Manuscript received April 28, 1982; revised July 13, 1982.
The author is with Philips Research Laboratories, Cross Oak Lane, Redhill, Surrey, RH1 5HA, England.

0018-9480/82/1100-1893$00.75 ©1982 IEEE

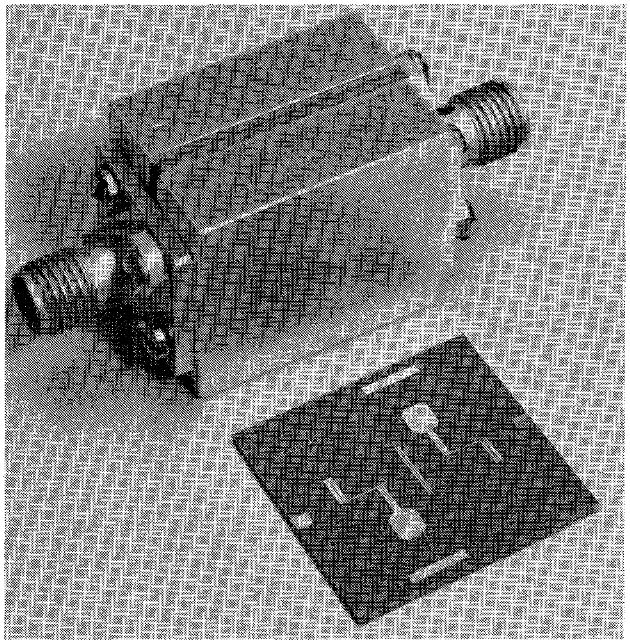

Fig. 2. 4–8-GHz bandpass filter.

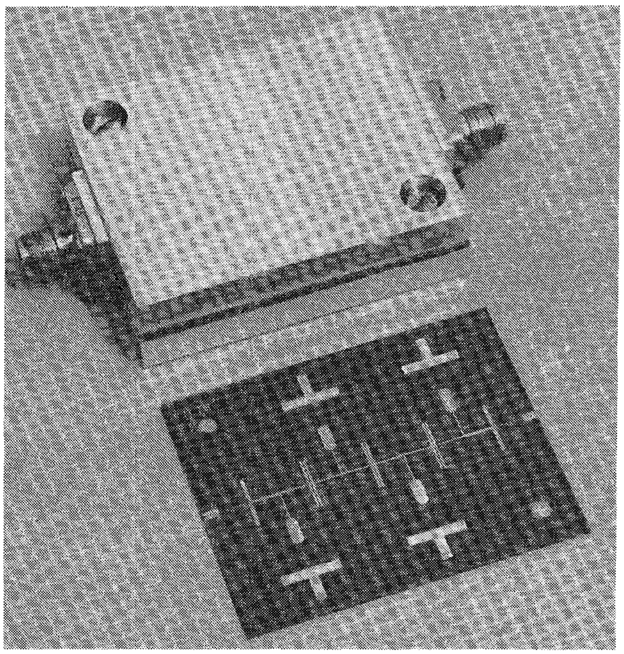

Fig. 3. 2–6-GHz bandpass filter.

circuits. Small lumped capacitors are required however, though these are easily mounted in place using thermal compression bonding equipment. The electrical performances of the filters are close to theoretical predictions and they are expected to meet the usual military environmental specifications.

II. Prototype Classification

The principle advantages of printed circuit filters are high repeatability and low cost in production. Once the photographic mask of a finished circuit is correct, a great number of near identical devices can be produced. However, in view of the relatively labor intensive and time-consuming aspects of producing the mask, it is important to achieve a final design with a minimum of iteration. It is therefore equally important to keep the circuit simple by striving 1) to avoid complicated sections consisting of multiple, capacitively coupled strips, and 2) to try to separate shunt or series elements with lengths of transmission line (unit elements in S-plane) so that each element corresponds to preferably one or no more than two transmission zeros. This helps in the association of an error in performance with a particular circuit element and in the confident determination of the necessary modification that must be made. It also ensures the most reliable stripline models are employed. In addition to keeping the circuit simple, short circuits must be avoided if at all possible since these are difficult to make and are not easily adjusted.

Both the above practical considerations have a strong influence on the choice of transmission zero locations. Firstly, to provide the separation of shunt or series elements, approximately equal numbers of zeros at $S=1$ (corresponding to unit elements) and zeros on the jw axis should be specified. This also helps to keep the dynamic range of element values small. Secondly, to avoid short circuits and corresponding shunt inductors in the prototype, only a single transmission zero may be specified at $S=j0$. If the appropriate canonical form is chosen such that the input impedance $Z_{\text{in}}(S)$ tends to infinity at $S=j0$, then this ensures that the only high-pass elements which the prototype contains will be series capacitors. There can be more than one series capacitor resulting from partial pole removals from $Z_{\text{in}}(S)$.

Each of the four classes of prototype A, B, C, and D are consistent with the above constraints. They are defined as follows.

A. Class A

The network configuration for prototypes of this class is given in Fig. 4(a). It consists of an alternating cascade of the two basic sections shown in Fig. 4(b) and (c); the first, a BP section providing two half-order zeros at $S=1$ and contributing to single zeros of transmission at $S=j0$, and $S=j\infty$; the second, a fourth-order section providing a pair of first-order jw axis zeros, one at each side of the passband. The specification of all the transmission zeros is

$a=1$	number of zeros at $S=j0$
$b=1$	number of zeros at $S=j\infty$
$c=(p+1)\times 2$	number of zeros at $S=1$
$d=p$	number of zeros at $S=jw_{z1}$
$e=d$	number of zeros at $S=jw_{z2}$

where p is the number of fourth-order elements and the degree of the network is $2\times(3p+2)$.

Though not essential, it is strongly advisable to locate all the pairs of finite, nonzero transmission zeros (loss poles) at the same frequencies on both sides of the passband as this leads to a smaller dynamic range of element values. The precise location of the zeros should be chosen to be as close to the passband edges as is necessary to give the

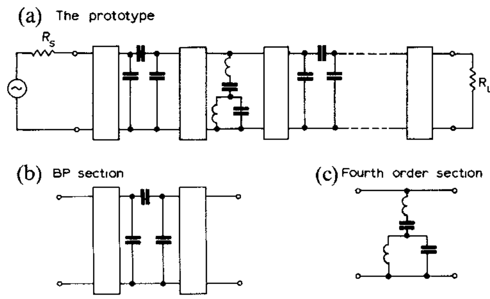

Fig. 4. The Class A prototype.

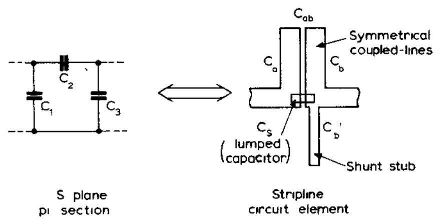

Fig. 5. Stripline circuit element for a pi section.

required skirt selectivity. It is also advisable to choose the zero locations so that they are equally displaced from the center frequency of the passband as this tends to assist the realization of the fourth-order elements. Finally, the realization of fourth-order elements is known to become more difficult as the zeros in the S-plane move away from $S = j1.0$ and are completely unrealizable if one of the zeros is specified below $S = j0.2$.

The unit elements of the network map directly into lengths of transmission line of the same value but scaled by the appropriate system impedance, usually 50 Ω. The capacitive pi sections are realized using stripline elements of the form shown in Fig. 5. When tight coupling is required, the total series coupling capacitance is shared between the edges of the strips (i.e., the distributed fraction) and a lumped capacitor mounted across the center of the section. The sharing of the coupling must be chosen to give an optimum combination of gap and capacitor dimensions. Mixing lumped and distributed elements in this way within all four classes of filter is only possible because of the lumped character of all the circuit elements at frequencies in the vicinity of the passband. A similar technique was used by Wenzel in designing combline filters [4]. In addition, there are other important advantages to be gained from this property, to which further reference will be made in Section IV-B.

Each fourth-order element is realized in one of two different forms depending on the location of the pair of transmission zeros each produces. As shown in 2) of Appendix I, the fourth-order element can be transformed into four-unit elements and realized as a cascade of four lengths of transmission line which would then appear in shunt with the 'main' line of the filter. From 3) in Appendix I, however, the fourth-order element can be transformed to consist of two second-order elements in parallel, each of which using 1) of Appendix I can be realized as a cascade of two lengths of line. It is the separation of the jw-axis zeros about the passband that will determine their realiza-

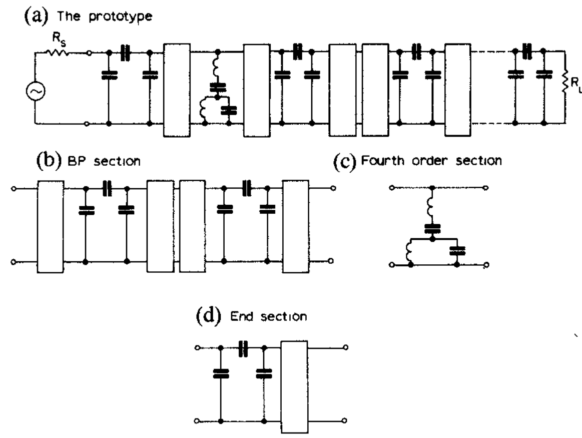

Fig. 6. The Class B prototype.

tion as either four lengths of line or as two double-length lines in parallel. The former will be found to be most appropriate for passband widths > 50 percent, especially if one of the transmission zeros is close to the minimum of $j0.2$. The latter will be most appropriate for passband widths < 50 percent. This will also depend to some extent on the stopband width since the stopband width affects the separation of the S-plane zeros. All lengths of transmission line in this and the other three classes of filter are a quarter-wavelength at f_s, the center frequency of the stopband.

Broadly speaking, filters of this class are realizable for fractional bandwidths in the range 50–100 percent and for stopbands specified up to seven times the center frequency of the passband. However, in general, the realization problem is eased as the specified stopband width decreases and it may be possible to realize devices for bandwidths outside the above range if a small stopband width is acceptable. It should be noted that choosing a stopband width such that the second passband is as low as even three times the center frequency of the first (i.e., $m = 3$) could still be worthwhile since the physical realization may be smaller or more desirable than a conventional filter design with the same performance.

It will usually be necessary to scale the internal impedance of the complete network by adjusting the symmetry of the two outermost pi sections. This is easily achieved using Y matrix transformations or the simple equations given in (4) and (5) in Appendix I. For narrowband cases, it may also be necessary to move some series and/or shunt capacitances through the end-unit elements using Kuroda identities, but this should be avoided if possible since it is convenient to begin the circuit at both ends with a length of transmission line. Indeed, it is one of the most significant advantages of this class of filter that a design can be produced with a simple length of line at the input and without the addition of redundant unit elements.

B. Class B

The network configuration for prototypes of Class B is shown in Fig. 6. It consists of an alternating cascade of the two basic sections shown in Fig. 6(b) and (c) between end sections of the type shown in Fig. 6(d). Fig. 6(b) provides four half-order transmission zeros at $S=1$ and contributes to single zeros at $S=j0$ and $S=j\infty$. Fig. 6(c) is a fourth-order section which, as in Class A, provides first-order zeros on each side of the passband. The end sections are a result of moving a series inductor and capacitor through a redundant unit element at each termination and the unit element does not, therefore, correspond to an extra transmission zero at $S=1$. The specification of all the transmission zeros is

$a=1$	number of zeros at $S=j0$
$b=1$	number of zeros at $S=j\infty$
$c=(p-1)\times 4$	number of zeros at $S=1$
$d=p$	number of zeros at $S=jw_{z1}$
$e=p$	number of zeros at $S=jw_{z2}$

where p is the number of fourth-order elements and the degree of the network is $2\times(4p-1)$.

Realization of the elements of these networks follows the same pattern as for Class A networks and the same considerations concerning the lumped capacitors, the fourth-order elements and the scaling of internal impedances must be made. However, one advantage and one disadvantage distinguish Class B from Class A networks. Class B networks are realizable over a considerable range of fractional bandwidths, a range which probably extends from below 10 percent up to around 100 percent for m (see Fig. 1) specified up to 7. This versatility is a worthwhile advantage. The disadvantage is associated with the necessary introduction of a redundant unit element into each end of the network, which at the input end results in a loss of control of the phase of the reflection coefficient. This may not be acceptable especially if more than one such filter is to be designed with a view to a parallel connection at a common junction in a multiplexer.

C. *Classes* C *and* D

Both these classes of prototype will be described together for the sake of brevity. They are in effect duals of the capacitively loaded interdigital filter. Their network configurations are described in Figs. 7 and 8, respectively, and their similarity is at once apparent. In fact, they are distinct from each other in respects similar to those distinguishing Classes A and B, namely:

1) Class C types are most suitable for broadband applications where fractional passband widths are > 50 percent, while Class D types are most suitable for bandwidths of an octave or less.

2) Class C types usually do not require the introduction of redundant unit elements at each end of the network and therefore do not incur the associated disadvantages. Class D types necessitate the introduction of unit elements.

Class C types are an alternate cascade of unit elements and capacitive pi networks. The set of transmission zeros are specified

$a=1$	number of zeros at $S=j0$
$b=q$	number of zeros at $S=j\infty$
$c=q+1$	number of zeros at $S=1$

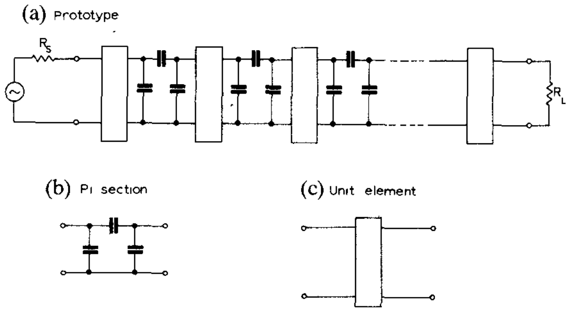

Fig. 7. The Class C prototype.

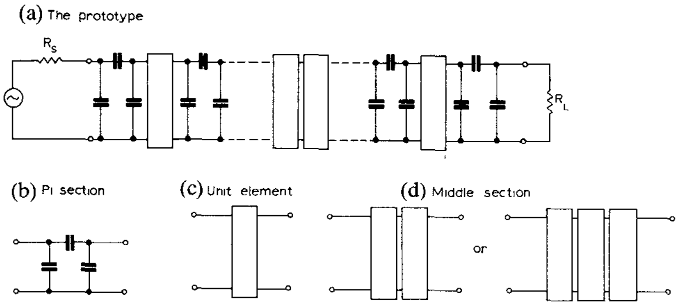

Fig. 8. The Class D prototype.

where q is the number of transmission zeros at infinity and the degree of the network is $2\times(q+1)$. Class D types can be derived from the exact network dual of the capacitively loaded interdigital filter. Their networks differ from the Class C networks in the center and at each end. Their transmission zeros are specified

$a=1$	number of zeros at $S=j0$
$b=q$	number of zeros at $S=j\infty$
$c=q-1$	number of zeros at $S=1$

where q is the number of transmission zeros at infinity and the degree of the network is $2\times q$. The dual of the interdigital filter includes series inductors between each unit element, and the absence of either one or two pi sections in the center of the D networks is a result of moving all the series inductors out from the center through the adjacent unit element. Two pi sections will be absent from the center if the degree of the network is divisible by 4.

Realization of the elements of these prototypes is the same as for the corresponding elements in Class A and B prototypes. Unit elements map directly to lengths of transmission line and the pi sections map to pairs of capacitively coupled strips which may or may not require the addition of a lumped capacitor. In fact, it is likely that for narrowband (< 20 percent) Class D types, the distributed coupling between the strips will be adequate and no lumped capacitors will be required throughout the circuit.

III. Calculations of Circuit Dimensions

It is assumed that filters are to work into a 50-Ω load and source impedances and, therefore, all the normalized element values of the prototypes must be scaled accordingly. The three basic physical elements to be considered are then the simple length of transmission line, the capacitively coupled lengths of line, and the lumped capacitor.

Each unit element value in the prototype will usually correspond to the characteristic impedance of a simple length of line in the stripline circuit. The width of these lines is calculated using Cohn [5], allowing for a finite thickness of metalization. As mentioned in Section II-A, each pi section of the prototype will correspond to a stripline circuit of the form shown in Fig. 5. The shunt stub in the circuit enables an asymmetrical pi section to be realized with a symmetrical pair of coupled-lines. This is an important facility since accurate models for asymmetrical coupled-lines are not readily available in the literature. The innermost pi sections, which are usually symmetrical, will not require the extra stubs. Distributed capacitances and the value of the lumped capacitor for Fig. 5 are given by

$$\begin{aligned} C_a &= aC_1 \quad & C_b' &= a(C_3 - C_1) \\ C_b &= C_a \quad & C_s &= \frac{(C_2 - C_{ab}/a)\tan(\pi f_0/2f_s)}{2\pi f_0} \\ & & Z_s &= a/C_b'\Omega \end{aligned} \tag{1}$$

where C_a, C_{ab}, C_b, and C_b' are distributed capacitances normalized to ϵ, C_1, C_2, and C_3 are the values of the S-plane elements normalized to 50 Ω, C_s is the value of the lumped capacitor, $a = 377/\epsilon_r$ and where ϵ and ϵ_r are absolute and relative permittivities, respectively.

C_{ab} should be chosen somewhere in the range 1–2.5 to give a desirable gap between the coupled strips. The coupled-strip dimensions are then derived from C_a and C_{ab} using Cohn's papers [6], [7]. The shunt stub dimensions are derived from Z_s using Cohn [5]. The lumped capacitor consists of a 5-μ thick strip of gold foil, thermocompression bonded to one of the coupled strips, and insulated from the adjacent strip with a thin film of dielectric material as shown in Fig. 9. The strip forms a square, parallel-plate capacitor whose linear dimension is

$$1 = \sqrt{(C_s \times d)/\epsilon} \tag{2}$$

where d is the thickness of the dielectric and ϵ is the permittivity of the dielectric.

Lines and stubs throughout the circuit are required to be an electrical quarter-wavelength at the chosen stopband center frequency f_s. The corresponding physical length is easily calculated knowing the phase velocity in the relevant dielectric material but the effects of edge capacitances and junctions at the ends of real resonators necessitate the application of corrections. For junctions, the main objective is to determine the position of the reference plane for each radial arm and some guidance for this can be obtained from [8, ch. 5]. Junction susceptance will not usually present a problem unless the junction area is excessively large, in which case an attempt should be made to remove it by removing an appropriate quantity of conductor material from the junction. This type of discontinuity is indeed difficult to characterize/model in the general case, but satisfactory results can be obtained quickly by experiment. For edge capacitances, length corrections are made

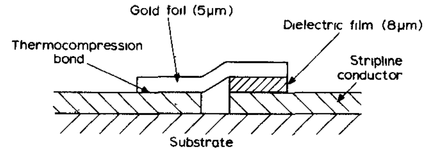

Fig. 9. Construction of lumped capacitors in stripline.

using

$$\Delta l = \frac{\lambda}{4}\left[1 - \frac{2}{\pi}\tan^{-1}\left\{\frac{Y_0}{2\pi f_0 C_f}\right\}\right] \tag{3}$$

where Δl is the reduction in length required, λ is the wavelength in the substrate at f_0, C_f is the total fringing capacitance at the relevant edge, and Y_0 is the characteristic admittance of the resonator. If the resonator is one of a pair in a capacitively coupled section then Y_0 is taken to be Y_{0e}, where Y_{0e} is the even mode characteristic admittance for the section.

IV. Design Examples

The 4–8 GHz and 2–6-GHz filters are derived from Class A prototypes and have stopbands which extend beyond 20 GHz. Specifications and expected and measured responses are presented for both filters, but owing to their intrinsic similarity, details of the design procedures will be given for only the 4–8-GHz device.

A. Specifications

The electrical specifications of the two filters are as follows.

1) 4–8 GHz Filter:

Insertion loss < 1.0 dB, 4–8 GHz
Insertion loss > 45 dB, 0–3.6 and 8.4–25 GHz
Passband ripple 0.1 dB for 15 dB return loss.

2) 2–6-GHz Filter:

Insertion loss < 1 dB, 2–6 GHz
Insertion loss > 65 dB, 0–1.8 and 6.2–20 GHz
Passband ripple 0.1 dB for 15 dB return loss.

B. 4–8-GHz Filter Design Details

A Class A prototype was chosen to meet the high skirt selectivity required and the possibility of a future multiplexer application. Two pairs of transmission zeros were provisionally placed at 3.5 and 8.5 GHz, respectively, which, referring to Section II-A, results in an overall degree of 16. An arbitrary choice of $m = 5$ gives zero locations in the S-plane of

1 at $S = j0$
1 at $S = j\infty$
2 at $S = j0.3153$
2 at $S = j0.9163$
6 at $S = 1.0$

and passband edges of

$$S = j0.364$$
$$S = j0.839.$$

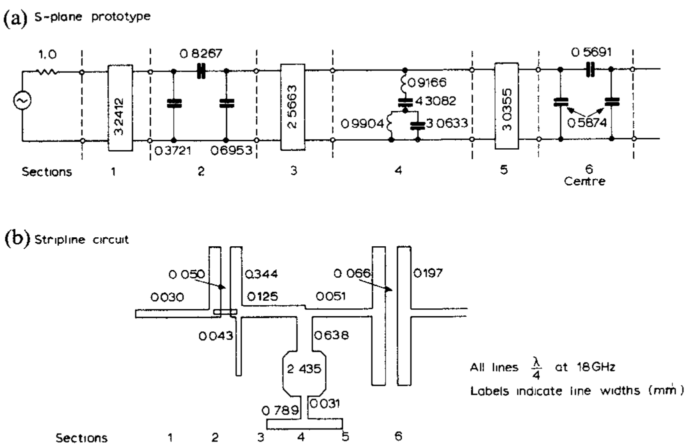

Fig. 10. 4–8-GHz filter—Equivalent circuits. (a) S-plane prototype. (b) Stripline circuit.

The basic network was then synthesized using these zero locations. On analysis, its frequency response was found to meet the specifications of Section IV-A-1, and only minor modifications were required for the network to be physically realizable. The final form of the transformed prototype is given in Fig. 10(a). Being symmetrical, only half of the network need be shown.

Fig. 10(b) gives an outline sketch of half of the stripline circuit and the dimensions of the individual stripline elements. The range of line and gap widths required in this design does stretch the capabilities of the photolithographic technology, but a number of these devices have been made without difficulty and it should be possible to reduce the range of the dimensions in future designs. Indeed, the smallest gap and line dimensions in the 2–6-GHz filter were nearer 100 μ. The dimensions apply to a circuit constructed using 1/32-in thick RT Duroid 5870 material with a dielectric constant of 2.32 and a 1/2-oz copper cladding. All the lines are a quarter-wavelength at 18 GHz and suitable length corrections have been applied to allow for the effects of junctions and end capacitances. In addition to the length corrections, it was necessary to remove the corners from the wide sections of the fourth-order elements so as to compensate for the large discontinuity capacitance at each end. Because of the lumped character of the elements around the frequency of the passband, such discontinuities are easily treated by assessing the excess capacitance of the section from insertion loss measurements. The excess is then removed by suitable trimming. In the case of the fourth-order elements, it is the position of the transmission zero above the passband which determines what changes must be made to the wide sections.

The value of the lumped capacitors required for the end coupled strips was calculated to be 0.146 pF. Using a dielectric film of Kapton (a polyimide) with a thickness of 0.008 mm and a dielectric constant of 3.0, (2) gives the linear dimension of the square patch as 0.210 mm.

It is worth noting that sections with what would be considered unacceptable aspect ratios in more conventional filter designs can usually be accommodated in these classes of filter. Furthermore, the task of fine tuning these filters in the final stages of a design is particularly easy. Again, the lumped character of the circuit elements is responsible for both these significant advantages. As far as the passband is concerned, any shunt element can be considered as requiring a particular shunt capacitance and an excess can be compensated by reducing either the length or the width of the element.

C. Results

The measured and theoretical insertion loss responses of the 4–8 GHz filter are given in Fig. 11. Outside the passband, the measured response can be seen to track the theoretical response with admirable precision and no further passband can be observed above the noise floor of the measurement system up to 18 GHz. Inside the passband the insertion loss is mostly under 1 dB but rising to a less attractive figure of approximately 3 dB at the passband edges. Return loss measurements in the passband of the filter suggest that some of this loss is due to reactive mismatches and it should, therefore, be possible to reduce the losses by further circuit trimming/tuning. However, additional practical experiments have indicated that a high proportion of the losses are copper losses which in turn are associated with the narrow gaps between capacitively coupled lines. They can be reduced by silver plating the circuits and/or using a larger ground-plane spacing and it is estimated that after suitable circuit trimming it should be possible to reduce inband losses to nearer 0.5 dB, rising to 2 dB at the passband edges. It must be stated that this 2-dB figure refers to the loss at the edge of a passband defined by the passband ripple, and if such a figure is unacceptable for the edge of a real passband, a filter should be designed with a ripple bandwidth slightly greater than that which is called for in the specification.

The measured and theoretical insertion-loss responses of the 2–6-GHz filter are given in Fig. 12. There is exceptionally close agreement between theory and practice. Throughout the stopband, attenuation is in excess of the noise floor of the basic measurement system used to test the 4–8-GHz filter, and to verify that the stopband rejection was greater than that called for in the specification, the 2–6-GHz filter was tested on a more sensitive system. The rejection throughout the stopband is greater than the now lower noise floor of approximately 65 dB. Insertion loss is considerably lower than 1 dB over most of the passband and as low as 0.6 dB in the center. The loss at the 2- and 6-GHz corner frequencies is around 6 dB, indicating that the passband width is fractionally narrow but the error in width can only be of the order of a few megahertz in view of the extreme slope of the filter skirts. It should not be difficult to reduce this figure by further circuit trimming and by increasing the ripple bandwidth slightly, as previously suggested. Even allowing for the 6-dB loss at 2- and 6 GHz, the present design results in a device with an exceptional performance in the triplate medium. As practi-

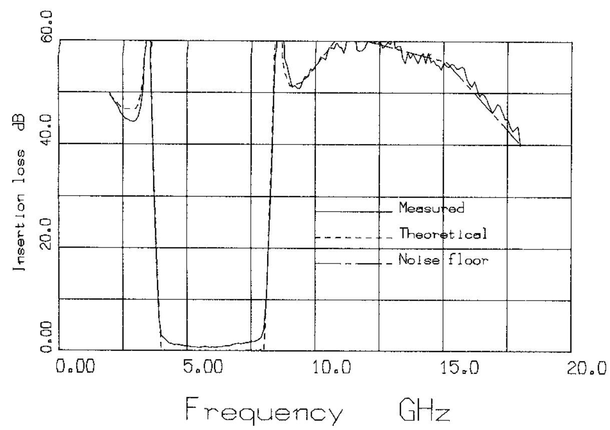

Fig. 11. Insertion-loss characteristics of the 4–8-GHz device.

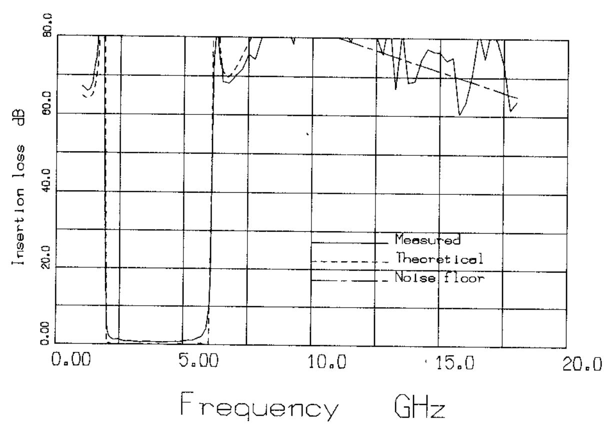

Fig. 12. Insertion-loss characteristics of the 2–6-GHz device.

cal evidence of the ease with which such circuits are tuned, only one single iteration was required after definition of the first photographic mask.

Both the 4–8-GHz and 2–6-GHz devices and all the four classes of filter that have been described should have no difficulty in meeting military environmental specifications. To check at least the temperature stability of the devices, the 4–8-GHz filter has been temperature cycled between −20 and +80°C. There was less than 0.05 percent peak drift in the passband center frequency and the center frequency returned to its original value at the ambient room temperature after the experiment.

V. Conclusions

The growth in the power and distribution of small and inexpensive computers will undoubtedly result in a more widespread use of exact synthesis procedures for microwave filters. This potential can be heavily exploited by the identification of the four classes A, B, C, and D of BP prototypes that have been described. The prototypes are synthesized from a simple specification of transmission zero locations and together the classes cover most of the pass and stopband requirements likely to be encountered in microwave receiver systems. They are particularly suitable, however, for broadband, highly selective filters with wide stopbands.

Physical realization in triplate is simple, inexpensive, and ideal for applications which require close amplitude and phase tracking of a batch of devices. The tuning of all the elements to resonate well above the passband also results in an exceedingly small device.

The first two of what now number five different and successful Class A devices have been described, both of which perform close to theory. Though no examples of Class B, C, or D devices have been constructed, their ranges of realizability have been otherwise thoroughly investigated.

Appendix I
The Following Network Transformations Will Be Relevant.

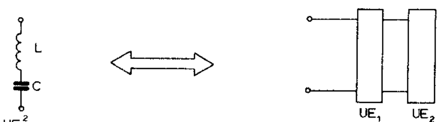

$$L = \frac{UE_1^2}{UE_1 + UE_2} \qquad UE_1 = L + \frac{1}{C}$$

$$C = \frac{UE_1 + UE_2}{UE_1\, UE_2} \qquad UE_2 = \left(L + \frac{1}{C}\right)\frac{1}{LC}$$

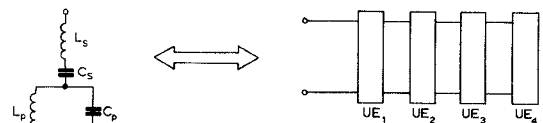

$$YE_i = \frac{1}{UE_i}$$

$$C_S = YE_1 + YE_2 + YE_3 + YE_4 \qquad YE_1 = \frac{C_S\left(L_pC_p + 1\right)}{\left(L_pC_p + 1\right)\left(1 + C_SL_S\right) + C_SL_p}$$

$$\frac{1}{L_S} = \frac{YE_1}{YE_2}\left(YE_1 + YE_2 + \frac{YE_1YE_3}{YE_2YE_4}\left(YE_3 + YE_4\right)\right)$$

$$YE_2 = \frac{YE_1^2\left(C_pL_S - \frac{1}{L_pC_S}\right) + \frac{YE_1}{L_p}}{YE_1\left(1 + \frac{L_S}{L_p} + \frac{C_p}{C_S} + \frac{2}{L_pC_S}\right) - \frac{1}{L_p}}$$

$$n^2 = \frac{YE_2}{YE_1} + \frac{YE_4}{YE_3} + \left(\frac{YE_1 + YE_2}{YE_1\, YE_2}\right)\left(YE_3 + YE_4\right) - C_SL_S - \frac{YE_2YE_4}{C_SL_SYE_1YE_3}$$

$$YE_4 = \frac{C_S - YE_1 - YE_2}{\left(\frac{YE_2}{L_SC_SL_pC_pYE_1} + 1\right)}$$

$$C_p = \frac{YE_2YE_4}{n^2L_SYE_1YE_3}$$

$$L_p = \frac{n^2}{C_S} \qquad YE_3 = C_S - YE_1 - YE_2 - YE_4$$

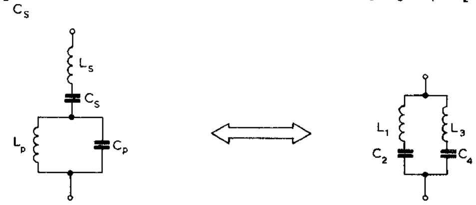

$$L_S = \frac{L_1L_3}{L_1 + L_3}$$

$$\omega_{01,2}^2 = \frac{\left(C_pL_p + C_SL_S + L_pC_S\right) \pm \sqrt{\left(C_pL_p + C_SL_S + L_pC_S\right)^2 - 4C_pL_pC_SL_S}}{2C_pL_pC_SL_S}$$

$$C_S = C_2 + C_4$$

$$L_p = \frac{L_1C_2 + L_3C_4}{C_2 + C_4} - \frac{C_2C_4\left(L_1 + L_3\right)}{\left(C_2 + C_4\right)^2} - \frac{L_1L_3}{L_1 + L_3} \qquad L_1 = \frac{L_S\left(1 - \left(\frac{\omega_{02}}{\omega_{01}}\right)^2\right)}{1 - L_SC_S\omega_{02}^2}$$

$$C_p = \frac{C_2C_4\left(L_1 + L_3\right)}{L_p\left(C_2 + C_4\right)} \qquad C_2 = \frac{1}{L_1\,\omega_{01}^2}$$

$$L_3 = \frac{L_S\left(1 - \left(\frac{\omega_{01}}{\omega_{02}}\right)^2\right)}{1 - L_SC_S\,\omega_{01}^2}$$

$$C_4 = \frac{1}{L_3\,\omega_{02}^2}$$

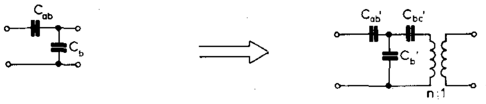

$C_{ab}'=\frac{C_b C_{ab}}{C_b+C_{ab}(1-n)}$ $\quad C_b'=\frac{C_b}{n}$ $\quad C_{bc}'=\frac{C_b}{n(n-1)}$

For $C_{ab}'=C_{bc}'$ make $n=\sqrt{1+\frac{C_b}{C_{ab}}}$

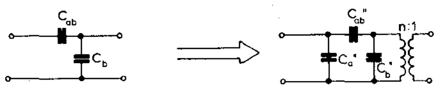

$C_a'=C_{ab}\left(1-\frac{1}{n}\right)$ $\quad C_{ab}''=\frac{C_{ab}}{n}$ $\quad C_b''=\frac{1}{n}\left(\frac{C_b}{n}+C_{ab}\left(\frac{1}{n}-1\right)\right)$

For $C_a'=C_b'$ make $n=\sqrt{1+\frac{C_b}{C_{ab}}}$

Acknowledgment

The author wishes to extend his thanks and appreciation to B. Hoad and R. S. Watts for their skilled assistance in the construction of laboratory models.

References

[1] P. I. Richards, "Resistor-transmission line circuits," *Proc. IRE*, vol. 36, pp. 217–220, Feb. 1948.

[2] M. C. Horton and R. J. Wenzel, "General theory and design of optimum quarter-wave TEM filters," *IEEE Trans. Microwave Theory Tech.*, vol. MTT-13, pp. 316–327, May 1965.

[3] H. J. Orchard and G. C. Temes, "Filter design using transformed variables," *IEEE Trans. Circuit Theory*, vol. CT-15, pp. 385–408, Dec. 1968.

[4] R. J. Wenzel, "Synthesis of combline and capacitively loaded interdigital bandpass filters of arbitrary bandwidth," *IEEE Trans. Microwave Theory Tech.*, vol. MTT-19, pp. 678–686, Aug. 1971.

[5] S. B. Cohn, "Characteristic impedance of shielded strip transmission line," *IRE Trans. Microwave Theory Tech.*, vol. MTT-2, pp. 52–55, July 1954.

[6] S. B. Cohn, "Shielded coupled-strip transmission line," *IRE Trans. Microwave Theory Tech.*, vol. MTT-3, pp. 29–38, Oct. 1955.

[7] S. B. Cohn, "Thickness corrections for capacitive obstacles and strip conductors," *IRE Trans. Microwave Theory Tech.*, vol. MTT-8, pp. 638–644, Nov. 1960.

[8] G. L. Matthaie, L. Young, and E. M. T. Jones. *Microwave Filters, Impedance-Matching Networks and Coupling Structures.* New York: McGraw–Hill, 1964.

Brian J. Minnis was born in Sheffield, England, in 1953. He received the B.Sc. (honors) degree in electronics from the University of Kent at Canterbury in 1973.

After graduating, he joined MEL at Crawley and worked on the design of various microwave components. At the end of 1974 he took up a post as Lecturer in Telecommunications at a college of further education in Hertfordshire. In 1976 he joined Marconi Space and Defence Systems at Stanmore and worked on the design of microwave antennas and radomes. Since 1978 he has been working at Philips Research Laboratories where his main field of interest has been broadband microwave filter design.

On Design and Performance of Lossy Match GaAs MESFET Amplifiers

KARL B. NICLAS, SENIOR MEMBER, IEEE

***Abstract*—The noise figure, the gain, and the reflection coefficients of lossy match amplifiers and their dependence on circuit elements are studied. Theoretical results are supported by measured data taken on a two-stage unit. In addition, the performance characteristics of a 100–8800 MHz four-stage lossy match amplifier are discussed. The unit exhibits 23.3 ± 1.1 dB of gain over the nearly 6-1/2 octaves. Its maximum noise figure is 10.9 dB from 100–8800 MHz and 6.6 dB from 2000–8000 MHz. The amplifier's overall circuit dimensions are 10×5.7 mm.**

I. Introduction

The BALANCED amplifier concept has dominated solid-state amplifier design for nearly two decades [1]. While it is expected to continue its dominating role, it will not go unchallenged by three single-ended amplifier concepts that have made great progress in the field of broadband amplification over the last few years. These three principles, which are presently competing for the best single-ended amplifier performance, are [2]–[7] 1) the matched feedback amplifier; 2) the lossy match amplifier; and 3) the distributed amplifier. They all are characterized by their compact size and, at least the first two by their simplicity and low cost. It is for these reasons that the matched single-ended amplifier concepts are very attractive whenever an economical solution to wide-band amplification is of primary concern.

The application of dissipative gain compensation in interstage matching networks [8] and amplifier stabilization by means of resistive-loaded shunt networks [9] have been

Manuscript received March 26, 1982; revised May 11, 1982.
The author is with the Watkins–Johnson Company, 3333 Hillview Avenue, Palo Alto, CA 94304.

0018-9480/82/1100-1900$00.75 ©1982 IEEE